Environmental Science and Pollution Research (2022) 29:32002–32015
https://doi.org/10.1007/s11356-022-18539-x

RESEARCH ARTICLE

Comparison of the toxicity of pure and samarium-doped zinc oxide nanoparticles to the green microalga *Chlorella vulgaris*

Sanaz Feizi[1] · Morteza Kosari-Nasab[1,2] · Baharak Divband[3] · Sepideh Mahjouri[4] · Ali Movafeghi[1]

Received: 8 June 2021 / Accepted: 3 January 2022 / Published online: 11 January 2022

Abstract

Although doping of various rare earth elements such as samarium on zinc oxide nanoparticles (ZnO NPs) can noticeably improve their photocatalytic performance, it may enhance their toxicity to living organisms. Thus, the toxic impacts of samarium-doped ZnO NPs (Sm/ZnO NPs) on different organisms should be carefully evaluated. In this study, an eco-toxicological experimentation system using the green microalga *Chlorella vulgaris* was established to determine the potential toxicity of ZnO and Sm/ZnO NPs synthesized by polymer pyrolysis method. Accordingly, growth parameters, oxidative stress biomarkers, and morphological features of the algal cells were analyzed. Both ZnO and Sm/ZnO NPs induced a concentration-dependent cytotoxicity by reducing the cell growth, decreasing photosynthetic pigment contents, and causing deformation in the cellular morphology. Moreover, generation of excessive H_2O_2, increased activity of superoxide dismutase and ascorbate peroxidase, and reduction in total phenolic and flavonoid contents were observed. Catalase activity was inversely influenced by the NPs in a way that its activity significantly increased at the concentrations of 20 and 25 mg L^{-1} of ZnO NPs, but was lessened by all supplemented dosages (5–25 mg L^{-1}) of Sm/ZnO NPs. Altogether, the obtained results revealed that Sm-doping can play a significant role in ZnO NP-induced toxicity on *C. vulgaris* cells.

Keywords *Chlorella vulgaris* · ZnO nanoparticles · Samarium doping · Oxidative stress · Cytotoxicity · Antioxidant enzymes

Introduction

ZnO nanoparticles (NPs) have acquired extensive interest in different industrial and biomedical fields due to their exceptional properties such as antimicrobial, antioxidant, and anticancer activities, along with low cost and low toxicity (Mishra et al. 2017). Furthermore, ZnO NPs possess wide band gap and high exciton binding energy, as well as excellent optical, electronic, and catalytic properties, making them the multifunctional materials for various industrial utilizations (Farooqi and Srivastava, 2016). The widespread manufacture of ZnO NPs and their post-use release in the environment affect ecosystem health. Consequently, the exposure risks of ZnO NPs to various organisms, especially aquatic organisms, are of particular concern. Previous studies have shown that ZnO NPs could be regarded as a threat to aquatic microorganisms through the formation of Zn^{2+} ions, which in turn generate reactive oxygen species (ROS) (Krzyżewska et al. 2016). It has been reported that different properties of ZnO NPs including size, shape, aggregation, and concentration can play a significant role in their hazardous activity in aquatic ecosystems (Krzyżewska et al. 2016; Peng et al. 2017). Furthermore, ZnO NPs have been proven to be toxic to various algal species at different concentrations. For instance, it has been identified that ZnO NPs (EC_{50} 1.94 mg Zn L^{-1}) were more toxic than bulk ZnO

Communicated by Bruno Nunes

✉ Sepideh Mahjouri
mahjouri@raberashidi.ac.ir

✉ Ali Movafeghi
movafeghi@tabrizu.ac.ir

1 Department of Plant Sciences, Faculty of Natural Sciences, University of Tabriz, Tabriz, Iran

2 Drug Applied Research Center, Tabriz University of Medical Sciences, Tabriz, Iran

3 Department of Inorganic Chemistry, Faculty of Chemistry, University of Tabriz, Tabriz, Iran

4 Department of Biological Sciences, Faculty of Basic Sciences, Higher Education Institute of Rab-Rashid, Tabriz, Iran

(EC_{50} 3.57 mg Zn L^{-1}) to marine chlorophyte *Dunaliella tertiolecta* (Manzo et al. 2013). The cytotoxicity evaluation of ZnO NPs with two hydrodynamic sizes (487.5 ± 2.55 nm and 616.2 ± 38.5 nm) towards freshwater algae *Scenedesmus obliquus* at low exposure concentrations (0.25, 0.5, and 1 mg L^{-1}) indicated that the smaller-sized ZnO NPs represented more toxicity. The released Zn^{2+} ions, ROS generation, and cell membrane damage, as well as adsorption and internalization of the NPs, were assumed to be contributed in the toxicity of algae cells (Bhuvaneshwari et al. 2015). A recent study has demonstrated that ZnO NPs not only can significantly inhibit *Microcystis aeruginosa* growth by imposing oxidative stress but also have a secondary effect caused by the release of intracellular toxins to the aquatic environment (Tang et al. 2018). Although a number of studies have already been conducted on the impact of NPs to aquatic microorganisms, it is quiet crucial to improve the information about the NP environmental risks to develop new strategies for their application.

Modifications of ZnO NPs, such as doping with different elements, offer an effective method to enhance and control some of their physicochemical properties. Particularly, doping various rare earth elements (REEs) on ZnO can noticeably improve their efficiency for various applications (Sin et al. 2013). Considering their wide optical band gap, REEs like Sm, Pr, Eu, Gd, and Nd can be applied as dopants to improve the nanostructure's electrical and optical properties (Kayani et al. 2020). It has been reported that Sm doping of ZnO nanomaterials not only enhanced the magnetic and optical properties but also led to the noticeable antibacterial activity. Moreover, it was suggested that Sm/ZnO can be considered as an appropriate candidate for application in tumor removal, pneumonia infection control, and malignant diseases treatment (Kayani et al. 2020). Another study has also revealed that application of Sm as dopants to ZnO NPs caused enhanced photoluminescence and antibacterial efficiency (Ravichandran et al. 2017). Remarkably, the synthesized Sm-doped spherical-like ZnO hierarchical nanostructures showed tremendous photocatalytic degradation of 2,4-dichlorophenol in comparison to the pure ZnO and commercial TiO_2 under visible light irradiation. Another advantage of these nanostructures is their easy separation and recycling capability, introducing them as promising structures for applications in environmental cleanup procedures (Sin et al. 2013). Although preferable benefits are expected from synthesis and modification of these types of NPs, there are serious concerns about their hazardous impacts on human health and the environment (Mahjouri et al. 2020). Hence, in addition to the physicochemical properties of the synthesized NPs, their biocompatibility and environmental safety should be carefully evaluated.

Microorganisms, as the main inhabitants of aquatic ecosystems, play foremost roles in primary productivity, nutrient cycling, and decomposition. It has been reported that microbial plankton communities in the aquatic environment are more vulnerable to NP toxicity. By causing cell and DNA damage as well as affecting reproduction, the toxicity of NPs can lead to adverse consequences in the environment (Zhu et al. 2019). On the other hand, the hazardous effects of NPs on microorganisms may have consequences on higher trophic levels, and hence it is crucial to determine the effect of NPs and their toxicity mechanisms on microorganisms. While the physiological and biological functions of microorganisms are adversely influenced by NPs, they also can accumulate and detoxify NPs (Gong et al. 2011; Nazari et al. 2018). Among the freshwater microalgae, *Chlorella vulgaris* has been commonly used as a model in eco-toxicological experiments (Xia et al. 2009). On account of its availability, culture requirements, and ease of use, *C. vulgaris* has been preferred to be applied in the experiments studying different types of potential toxicants (Silva et al. 2009). A number of previous studies have been evaluated the toxicity of ZnO NPs to this microalga. *C. vulgaris* treated with 50–300 mg L^{-1} of ZnO NPs for 24 h and 72 h showed a considerable decrease in the viability in dose and time-dependent manners. Besides, the changes detected in some biochemical markers such as the activity of SOD, GSH, LPO, and LDH confirmed the toxicity of ZnO NPs towards the algae (Suman et al. 2015). An investigation based on the chiral perturbation approach showed that ZnO NPs caused drastic changes in the amount of ROS in *C. vulgaris* and both released Zn^{2+} ions and the NPs contributed to the toxicity (Zhou et al. 2014). In another investigation, ZnO NPs induced the antioxidant defense system of *C. vulgaris* cells and the cell membrane and organelle damages, as well as oxidative stress were mentioned as the basic reasons for toxicity of the NPs to the algal cells (Saxena et al. 2021). To the best of our knowledge, this is the first report on the toxicity of Sm/ZnO NPs to microalga.

In this study, we conducted an eco-toxicological survey system using green microalga *C. vulgaris* to assess the toxic potential of pure and Sm/ZnO NPs synthesized by polymer pyrolysis method. First, the synthesized NPs were characterized by the combination of several techniques such as transmission electron microscopy (TEM), field emission scanning electron microscopy (FESEM), X-ray diffraction (XRD), energy dispersive X-ray (EDX), and dynamic light scattering (DLS). Subsequently, the impacts of pure and Sm/ZnO NPs on the green microalga *C. vulgaris* were analyzed by assessing growth parameters, oxidative stress biomarkers, and morphological features.

Materials and methods

Synthesis and characterization of pure and Sm-doped ZnO NPs

ZnO and Sm/ZnO nanoparticles were synthesized by using polymer pyrolysis method (Khatamian et al. 2012). At first, 0.8 mmol $Zn(CH_3COO)_2{\cdot}2H_2O$ was dissolved in 2 mL dilute nitric acid (2 mol L^{-1}), and then 1.6 mmol citric acid was added to the solution and stirred for 2 h. The pH was adjusted to 6–7 with dilute ammonia. Successively, the monomers of acrylamide (0.3 g) were supplemented to the clear solution. After stirring for 20 min, the obtained solution was placed in a water bath and heated to 80 °C. Afterward, polymerization occurred by addition of AIBN initiator ($C_8H_{12}N_4$) which resulted in a transparent polymeric resin with no precipitation. Finally, the obtained gel was dried at 100 °C for 24 h, then heated at 300 °C for 10 h and calcined at 550 °C for 5 h. Sm/ZnO NPs were produced by the same process with an extra step, which was the addition of 0.06 mmol of Sm_2O_3 into the Zn salt solution and stirring for another 2 h to acquire 15% Sm-doped ZnO NPs.

Structural and morphological characterization of the pure and Sm/ZnO NPs were determined by a combination of several techniques. The structure, average size, morphology, and elemental composition of the synthesized NPs were examined by XRD (Siemens D500, Germany), TEM (JEOL JEM- 2200FS, Japan), and FESEM (Hitachi S-4200, Japan) equipped with EDX. Average hydrodynamic diameters and zeta potential of the synthesized NPs were determined using DLS technique (Nanotrac Wave, Microtrac, USA).

Algal culture and treatments

The green microalga *C. vulgaris* CCAP 211/11B was obtained from Drug Applied Research Center of Tabriz University of Medical Sciences. For maintaining a stock culture, 50 mL of the algal cells was added to 200 mL of fresh, sterile BG-11 medium (pH 7) in 500-mL Erlenmeyer flasks (Rippka et al. 1979). The cultures were kept under cool white fluorescent lights (illumination intensity 5000 lx, photoperiod 16-h light and 8-h dark) with constant shaking at 25 °C and subcultured every 15 days. Toxicological experiments were directed in the exponential growth phase of algal cultures at day 7 of culture by using 100-mL Erlenmeyer flasks containing 50 mL of algal cell suspension. According to our preliminary experimental data, the NPs concentrations higher than 25 mg L^{-1} caused extreme algal cell death. Therefore, the cells were treated with different concentrations of ZnO and Sm/ZnO NPs including 0, 5, 10, 15, 20, and 25 mg L^{-1} and kept at the abovementioned condition. Three independent experiments as different replicates for analyzing the effect of each concentration of the NPs were conducted. After 24 h of incubation, algal cells were collected and stored at − 80 °C until use in different assays.

Scanning electron microscopy of algal cells

Scanning electron microscopy was used to observe the morphological modifications of treated cells. After 24 h of exposure to ZnO and Sm/ZnO NPs (20 and 25 mg L^{-1}), 25 mL of the cell suspensions were centrifuged and the acquired pellets were washed with BG-11 medium for several times to eliminate the unbound NPs. Subsequently, the treated and untreated algal cells were spread on a piece of aluminum foil and kept at − 20 °C for 24 h and then were freeze-dried for 1 h. Finally, the gold-sputtered samples were examined through FESEM (MIRA3 FEG-SEM) (Nazari et al. 2018).

Determination of cell growth

For analyzing the growth rate of algal cells, cell density was monitored using cell counting by a hemocytometer. Measuring the number of algae cell in the culture media after 0, 6, 8, and 24 h of exposure to the pure and Sm-doped ZnO NPs was achieved with a light microscope. Microscopic counts of the algal cells were repeated 3 times for each treatment of the NPs.

Measurement of photosynthetic pigments

To measure chlorophyll a, chlorophyll b, and carotenoids, 0.05 g (fresh weight) of treated and untreated algal cells were first crushed in liquid nitrogen and then homogenized in 1 mL of absolute methanol and stored for 24 h in darkness. After centrifuging for 10 min at 5000 *g*, the absorbance of the supernatant was determined at 470, 653, and 665 nm. The photosynthetic pigment content was calculated according to the following equations (Şükran et al. 1998).

$$C_a = 15.65A_{665} - 7.340A_{653}$$

$$C_b = 27.5A_{653} - 11.21A_{665}$$

$$C_{x+c} = 1000A_{470} - 2.860C_a - 129.2C_b/245$$

Quantification of hydrogen peroxide formation

Hydrogen peroxide (H_2O_2) content was evaluated by a spectroscopy method (Velikova et al. 2000). Accordingly, 0.05 g (fresh weight) of algal cells was crushed in liquid nitrogen

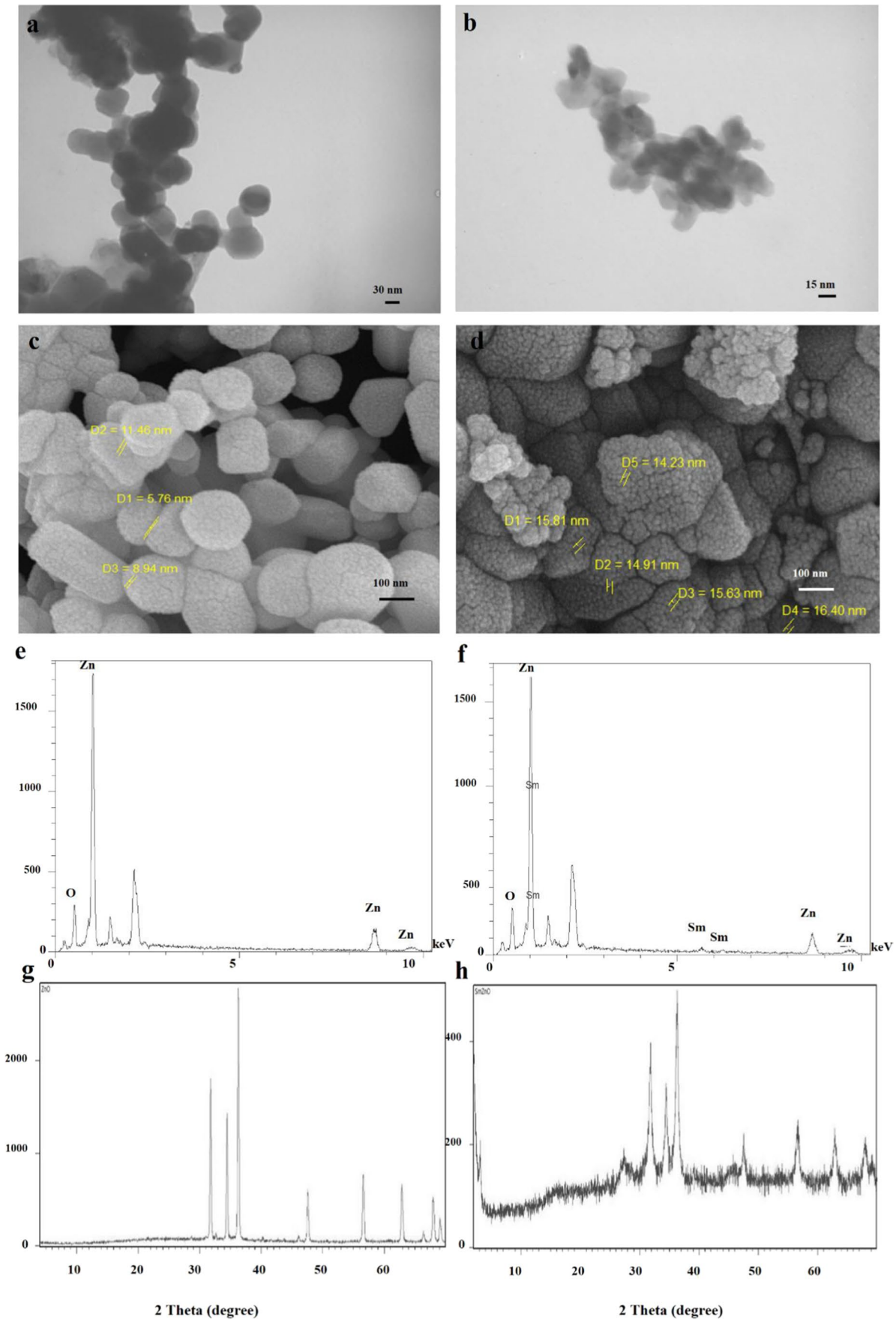
a
30 nm
b
15 nm
c
D2 = 11.46 nm
D1 = 5.76 nm
D3 = 8.94 nm
100 nm
d
D5 = 14.23 nm
D1 = 15.81 nm
D2 = 14.91 nm
D3 = 15.63 nm
D4 = 16.40 nm
100 nm
e
Zn
O
Zn
Zn
keV
f
Zn
Sm
O
Sm
Sm
Sm
Zn
Zn
keV
g
2 Theta (degree)
h
2 Theta (degree)

◂**Fig. 1** Scanning electron microscopy and transmission electron microscopy images of the synthesized NPs show the hexagonal-shaped NPs. TEM images of ZnO (**a**) and Sm/ZnO NPs (**b**). FESEM images of ZnO (**c**) and Sm/ZnO NPs (**d**). In the FESEM images, "D" represents diameter of the NPs. EDX spectra of ZnO (**e**) and Sm/ZnO NPs (**f**). XRD patterns of ZnO (**g**) and Sm/ZnO NPs (**h**)

and mixed with 1 mL of trichloroacetic acid (TCA, 0.1%) solution in a pre-cooled mortar and then was centrifuged at 10,000 *g* for 15 min at 4 °C. Subsequently, 0.5 mL of as-prepared supernatant, 0.5 mL of potassium phosphate buffer (10 mM, pH 7), and 1 mL of potassium iodide reagent (1 M) were mixed and stored for 15 min at 25 °C. The absorbance of the reaction mixtures was measured at 390 nm and H_2O_2 amount was determined as µg/g FW (fresh weight) using a standard curve.

Determination of antioxidant enzymes activities

For the determination of antioxidant enzyme activities, a quantity of 0.05 g (fresh weight) of cells was homogenized in liquid nitrogen and 0.05 M phosphate buffer (pH = 7). After centrifugation at 10,000 *g* for 15 min at 4 °C, the supernatant was used for analyzing protein concentration as well as ascorbate peroxidase (APX), superoxide dismutase (SOD), and catalase (CAT) activities. Total protein content was measured by Bradford method (Bradford 1976). SOD activity was investigated by inhibiting the photochemical reduction of nitro blue tetrazolium (NBT) by algal extract containing the enzyme according to the method described by Winterbourn et al. (Winterbourn et al. 1976). One unit of SOD was defined as the quantity of the enzyme inhibiting 50% of NBT reduction. Assessment of CAT activity was performed based on absorbance of the reaction solution containing 1.5 mL TS buffer (citrate–phosphate-borate) with pH = 7, 25 µL of algal extract, and 50 µL of hydrogen peroxide at wavelength of 240 nm for 3 min (Obinger et al. 1997). One unit of CAT activity was considered as equal to the amount of enzyme required to reduce 1 µmol of hydrogen peroxide per minute. APX activity was calculated using the method stated by Boominathan and Doran (Boominathan et al. 2002). The amount of enzyme needed for the oxidation of 1 µmol ascorbic acid/min was determined equal to the one unit of activity.

Measurement of total phenol and flavonoid content

The total phenol content of algal extracts was calculated using Folin-Ciocalteu reagent. For determining total phenol content, the methanolic extract of the algal cells (100 µL) was mixed with distilled water (2.5 mL) and then Folin reagent was added (100 µL). After 6 min, 150 µL of sodium carbonate 20% was added to the solution. After 30 min, absorbance of samples was read at 760 nm (Meda et al. 2005).

The total flavonoid content of the extracts was quantified by a colorimetric method reported by Chang et al. (2002). At first, 2 g of aluminum chloride ($AlCl_3$) was dissolved in 100 mL of methanol. Then, 500 µL of methanol solution containing aluminum chloride was added to 500 µL of the methanolic extract of algal cells. After 1 h, the mixture absorbance at 415 nm was recorded (Chang et al. 2002).

Statistical analysis

Statistical analysis was carried out by using a one-way analysis of variance (ANOVA) and means were compared using Duncan's multiple range tests at 5% level (SPSS16). All assays were conducted in triplicate. The results were expressed as mean ± standard error (SE). A *t* test was used to compare the means of two groups of experiments.

Results and discussion

Physicochemical characteristics of the NPs

TEM micrographs of the synthesized ZnO and 15% Sm/ZnO NPs by the polymer pyrolysis method showed the hexagonal-shape of NPs with the particle sizes of 15–45 nm and 15–35 nm, respectively. FESEM images confirmed that hexagonal-shaped ZnO and Sm/ZnO NPs are aggregated (Fig. 1a, b). The EDX patterns of the NPs displayed the existence of Zn and O elements in ZnO NPs structures as well as Zn, O, and Sm elements in Sm/ZnO NPs constructions. No impurity was evident in the elemental analysis of the samples (Fig. 1c, d). XRD patterns of pure and Sm-doped ZnO NPs exhibited main peaks representing a typical hexagonal wurtzite structure for the synthesized NPs (Fig. 1e, f). There were no diffraction peaks of Sm or other impurities in the XRD patterns revealing that Sm^{3+} ions are successfully doped on the ZnO structure. The observed diffraction peaks of the pure ZnO nanopowder were similar to those of hexagonal wurtzite ZnO (PCPDF79-0207). By adding Sm, a residual phase of Sm was notably detected by XRD (Fig. 1f). For identifying the behavior of NPs in the aqueous phase, their hydrodynamic particle size, polydispersity index (PDI), and zeta potential were measured in distilled water by DLS technique (Fig. 2). The average hydrodynamic diameter of ZnO and Sm/ZnO NPs were determined to be 63.97 nm and 81.6 nm, respectively. Sm has more water coverage because of positive charges, and as a consequence, the size of Sm/ZnO NPs was recognized slightly larger than ZnO NPs. Zeta potential for the synthesized NPs were measured as − 14 mV and − 9.54 mV for ZnO and Sm/ZnO NPs, respectively. Higher quantities of

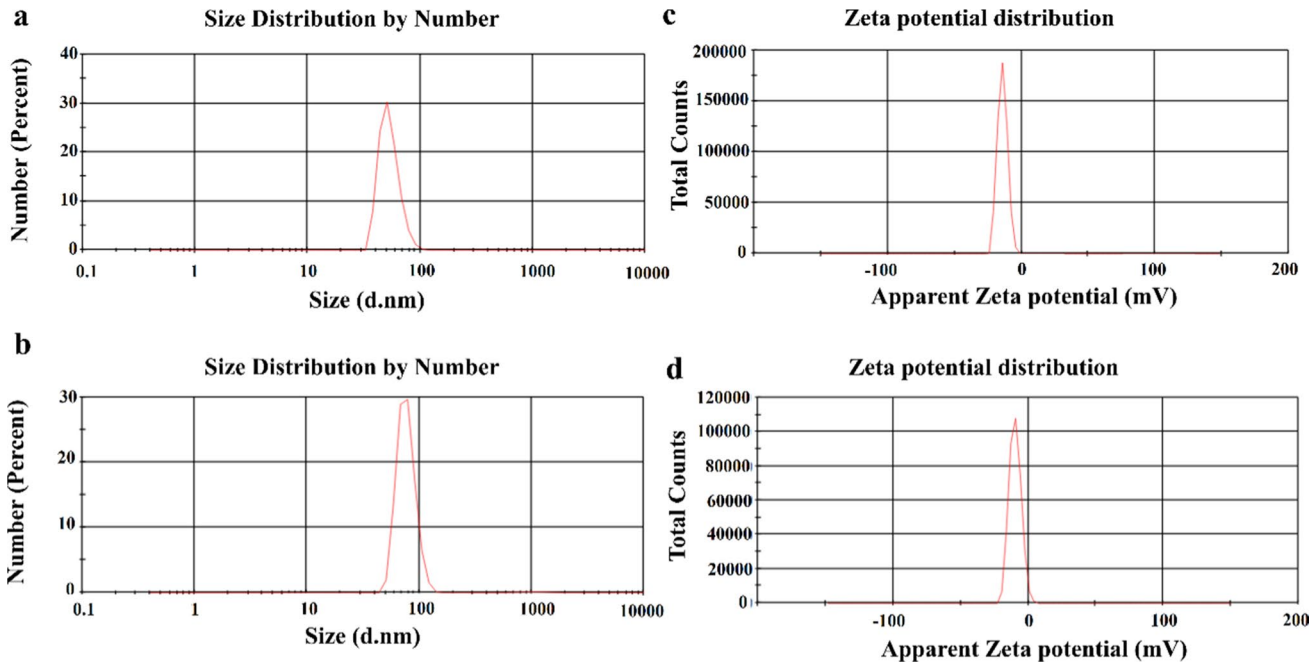

Fig. 2 DLS analysis determined the particle size distribution and zeta potential of ZnO (**a**, **c**) and Sm/ZnO NPs (**b**, **d**)

zeta potential for both NPs confirmed the stability of NPs in the suspension. Additionally, both NPs showed low PDI values, i.e., 0.30 for ZnO NPs and 0.48 for Sm/ZnO NPs, demonstrating their good dispersion in water media. According to the characteristics of the produced NPs including low size and good colloidal stability, they could be suitable for the purposes of the current study.

Growth and morphology of *C. vulgaris*

Growth responses of *C. vulgaris* to the different concentrations of pure and Sm-doped ZnO NPs (5–25 mg L^{-1}) were quantified using cell number ($\times 10^6$) per milliliter of medium after the exposure periods of 6, 18, and 24 h (Fig. 3a, b). In the control medium, cell number increased noticeably over the period of experiment. However, addition of the NPs to the culture media resulted in declining the growth of algal cells. Cell number lessened with the rising concentrations of both ZnO and Sm/ZnO NPs. Application of 25 mg L^{-1} of the NPs caused a rapid and significant decrease in cell number which was 70% for ZnO NPs and 78% for Sm/ZnO NPs after 24 h. Comparable results of the hazardous effect of ZnO NPs on *C. vulgaris* growth have been formerly reported (Zhou et al. 2014; Liu et al. 2018). ROS production and the released Zn^{2+} ions have been considered as the main reasons for cell and bacterial death in the studies evaluating ZnO NP toxicity. It has been reported that dissolution of ZnO NPs can affect the metabolism of cells and disrupt the function of the enzymatic system resulted in deterring cell growth and death (Carofiglio et al. 2020). According to the available data, REEs have been generally considered to be low toxic, but excessive REEs in the environment can act as pollutants and have adverse effects on different organisms (Goecke et al. 2015). It has been suggested that REEs can affect the growth of cells by nutrient depletion or disturbing the integrity of the biological membrane (Yuan et al. 2009; Kurvet et al. 2017). On the other hand, doping with REEs has been confirmed as a beneficial strategy to modify the antimicrobial properties of ZnO NPs (Carofiglio et al. 2020). It has been reported that Sm/ZnO NPs showed enhanced antibacterial efficiency compared with the undoped ZnO NPs. Doping of Sm on ZnO NPs can cause more release of Zn^{2+} ions, which can interact with the membrane of the exposed cells (Ravichandran et al. 2017; Kayani et al. 2020).

Our FESEM microscopic observations of control cells indicated an intact surface morphology (Fig. 4a, b). FESEM micrographs of treated *C. vulgaris* cells with both ZnO and Sm/ZnO NPs showed noticeable accumulation of the NPs on the cell surface (Fig. 4d, f). The algal cells treated with 25 mg L^{-1} of ZnO NPs for 24 h displayed surface deformations (Fig. 4c). In comparison, treated cells with 25 mg L^{-1} of Sm/ZnO NPs revealed robust cell lysis and injury as well as notable distortions in shape (Fig. 4e). Similar results have been already reported by Saxena et al. (2021) on *C. vulgaris* cells under exposure of 5 mg L^{-1} of ZnO NPs. Direct contact and aggregation of NPs on the external surface of algal cells possibly

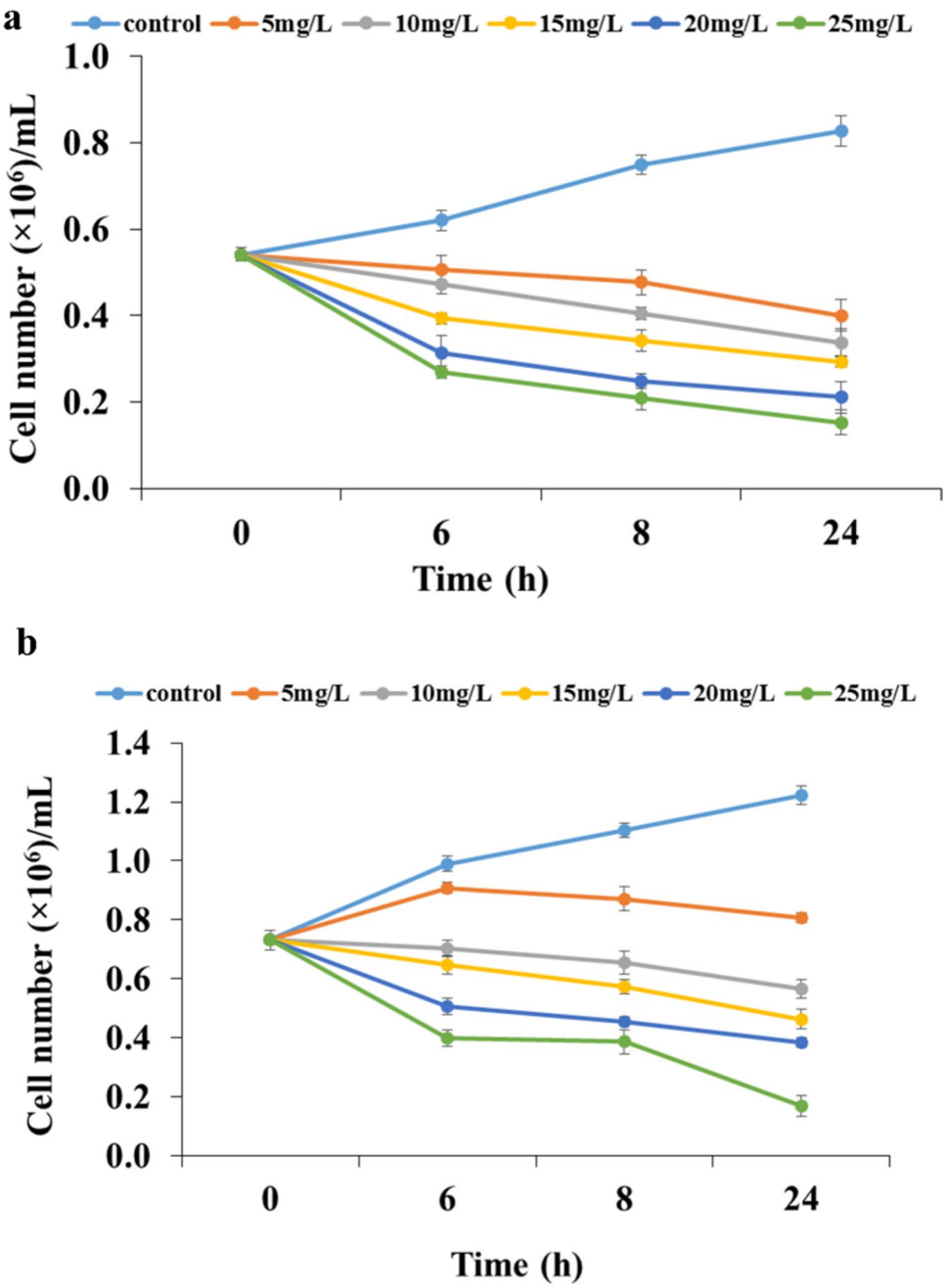

Fig. 3 The dose-dependent effects of ZnO (**a**) and Sm/ZnO (**b**) on algal cell number as a growth parameter after 6, 18, and 24 h of exposure. The results are presented as means ± SE ($n = 3$)

result in the particle-induced toxicity (Zhou et al. 2014). It is supposed that the adsorption of some metal oxide NPs on cell wall could be one of the possible mechanisms triggering the particle's toxicity to algal cells (Hoecke et al. 2009; Ma et al. 2015). Indeed, the direct interfacial interactions likely cause physical damages of the cell wall and cell membrane, and consequently lead to cell deformation as well as growth inhibition (Chen et al. 2012; Zhao et al. 2016). Moreover, the algal cells and NP heteroaggregations might indirectly influence the harmfulness by reducing the accessibility of light, which is known as the shading effect (Ma and Lin, 2013; Cheloni et al. 2016).

Photosynthetic pigment content

Toxicity of ZnO and Sm/ZnO NPs were further analyzed by quantifying the photosynthetic pigments (chlorophyll a, b, and carotenoids). Exposure to low concentrations of ZnO NPs did not affect chlorophyll a and b contents in *C. vulgaris* cells, while high concentrations of ZnO NPs could significantly decrease the amounts of chlorophyll a and b (Fig. 5a, c). In contrast, all applied concentrations of Sm/ZnO NPs considerably decreased the amounts of chlorophyll a and b in comparison to the control sample, except for the concentration of 5 mg L^{-1} for chlorophyll a quantity (Fig. 5b,

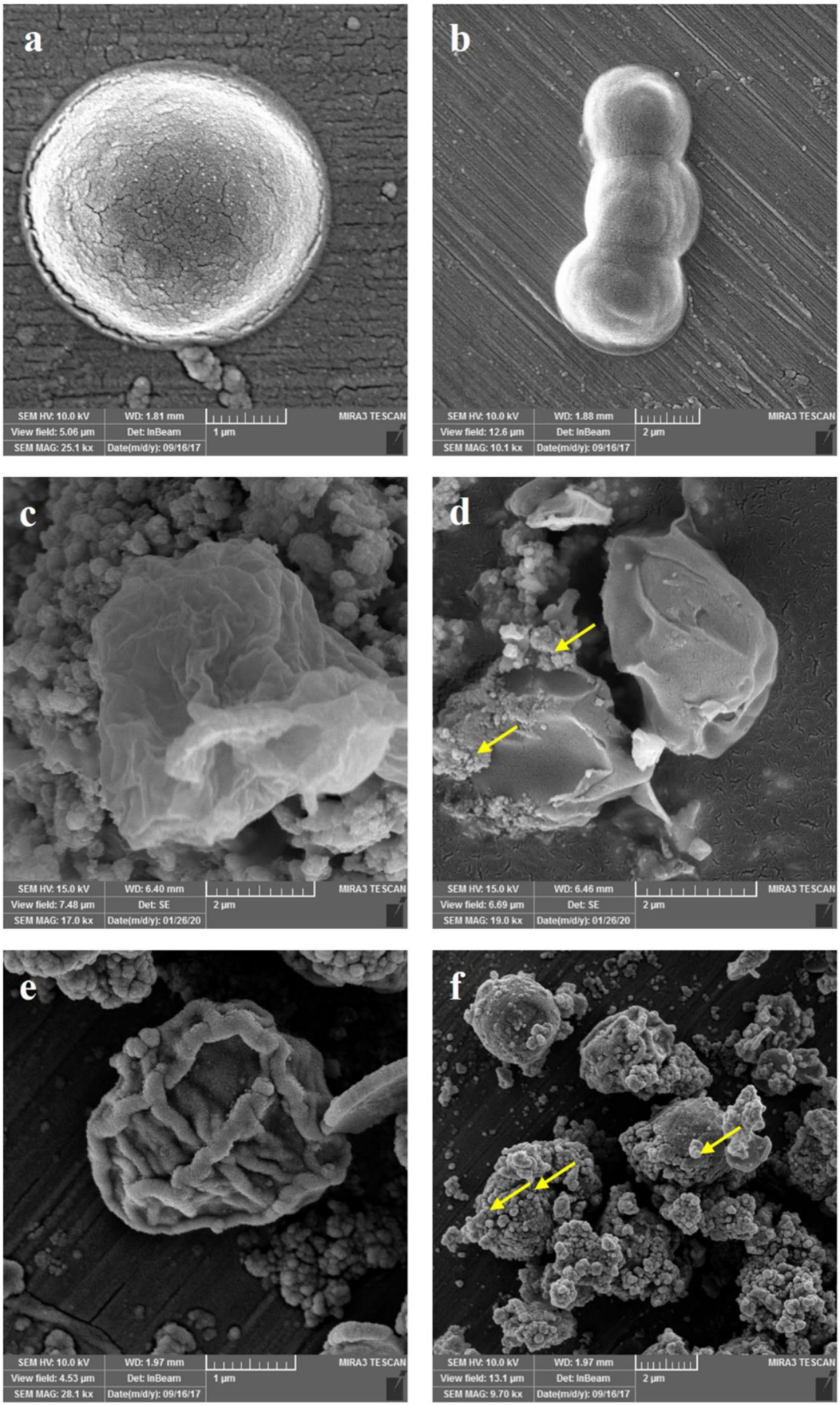
a
SEM HV: 10.0 kV
WD: 1.81 mm
MIRA3 TESCAN
View field: 5.06 µm
Det: InBeam
1 µm
SEM MAG: 25.1 kx
Date(m/d/y): 09/16/17
b
SEM HV: 10.0 kV
WD: 1.88 mm
MIRA3 TESCAN
View field: 12.6 µm
Det: InBeam
2 µm
SEM MAG: 10.1 kx
Date(m/d/y): 09/16/17
c
SEM HV: 15.0 kV
WD: 6.40 mm
MIRA3 TESCAN
View field: 7.48 µm
Det: SE
2 µm
SEM MAG: 17.0 kx
Date(m/d/y): 01/26/20
d
SEM HV: 15.0 kV
WD: 6.46 mm
MIRA3 TESCAN
View field: 6.69 µm
Det: SE
2 µm
SEM MAG: 19.0 kx
Date(m/d/y): 01/26/20
e
SEM HV: 10.0 kV
WD: 1.97 mm
MIRA3 TESCAN
View field: 4.53 µm
Det: InBeam
1 µm
SEM MAG: 28.1 kx
Date(m/d/y): 09/16/17
f
SEM HV: 10.0 kV
WD: 1.97 mm
MIRA3 TESCAN
View field: 13.1 µm
Det: InBeam
2 µm
SEM MAG: 9.70 kx
Date(m/d/y): 09/16/17

◂**Fig. 4** Effect of pure and Sm/ZnO NPs on the morphology of *C. vulgaris* cells. FESEM images of the control cells (**a**, **b**), algal cells after exposure to 25 mg L^{-1} of ZnO NPs (**c**, **d**), and Sm/ZnO NPs (**e**, **f**). The yellow arrows represent the agglomeration of NPs on the cell surfaces

d). Similarly, the total carotenoid content was reduced with exposure to 20 and 25 mg L^{-1} of ZnO NPs, although significant decreases were detected in all Sm/ZnO NP-treated cells, compared to the control sample (Fig. 5e, f). The effects of two types of NPs on the pigment contents were further compared using a *t*-test. All the calculated *t* values (all higher than 5.87) were greater than the critical *t* value, and thus there was a significant difference between the means of two groups of treatments ($df = 4$, $p \leq 0.01$). In other words, the applied concentrations of Sm/ZnO NPs had higher significant effects than the identical concentrations of ZnO NPs on the decrease of photosynthetic pigments in treated algae cells. Decrease of chlorophyll content in some algal cells has been reported after exposure to different concentrations of ZnO NPs (Djearamane et al. 2019; Kaliamurthi et al. 2019; Saxena et al. 2021). Based on the outcomes of our study, Sm-doping enhanced the effects of ZnO NPs on declining the chlorophyll and carotenoid contents. In the same way, it has been reported that treatment of *Microcystis aeruginosa* with 5 and 10 mg L^{-1} Nd^{3+} caused a significant drop in the chlorophyll a content after 8 days of exposure compared to the control sample (Yingjun et al. 2011). Molecular-based analysis of the toxicity of cerium oxide NPs to the freshwater alga *Chlamydomonas reinhardtii* revealed a downregulation of photosynthesis with related impacts on energy metabolism (Taylor et al. 2016). Photosynthetic pigments such as chlorophyll a, b, and carotenoids are efficient indicators of photosynthetic capacity in algal cells. Therefore, a reduction in the amount of these pigments indicates the decrease in photosynthetic efficiency which later can lead to growth arrest as was evident in our experiments.

Hydrogen peroxide content

To estimate the oxidative stress induced by ZnO and Sm/ZnO NPs, H_2O_2 level was measured in treated and untreated cells of *C. vulgaris* (Fig. 6a, b). According to the obtained results, the highest amounts of H_2O_2 were observed in the algal cells exposed to 25 mg L^{-1} of ZnO and Sm/ZnO NPs. Actually, the general toxic characteristic of different metal-based NPs is their ability to increase the generation of ROS, which subsequently results in oxidative stress. Therefore, the determination of ROS levels such as measuring H_2O_2 content can be used for analyzing the effect of NPs on the oxidative stress in phytotoxicological studies (Mahjouri et al. 2018). Based on our results, it can be suggested that the excessive production of H_2O_2 in the algal cells exposed to high concentrations of ZnO and Sm/ZnO NPs led to induction of oxidative stress permitting subsequent deterioration of photosynthetic efficiency and reduction in algal growth.

The response of enzymatic and non-enzymatic antioxidant defense systems

Oxidative stress induced by the different concentrations of ZnO and Sm/ZnO NPs (5–25 mg L^{-1}) were assessed by measuring the SOD, CAT, and APX activities in *C. vulgaris* cells (Fig. 7). After 24 h of exposure, SOD activity was significantly increased in the algal cells treated with 10–25 mg L^{-1} of ZnO NPs compared to the control samples. Similarly, high concentrations of Sm/ZnO NPs (15–25 mg L^{-1}) augmented the SOD activity in comparison to the control cells. A total of 25 mg L^{-1} of ZnO NPs and Sm/ZnO NPs led to a 2.6- and 1.9-fold increase in SOD activity, respectively (Fig. 7a, b). APX activity also varied considerably depending on the increase in the concentration of ZnO NPs. The treatments of 10–25 mg L^{-1} of ZnO NPs caused 1.7–2.1 times rise in the APX activity compared to the control samples. However, the highest APX activity of algal cells, approximately threefold higher than the control samples, was observed after exposure to 20 and 25 mg L^{-1} of Sm/ZnO NPs (Fig. 7c, d). CAT activity analysis in the treated algal cells with ZnO NPs indicated that the applications of both concentrations of 20 and 25 mg L^{-1} led to higher enzyme activity in comparison to the control samples. However, a significant concentration-dependent decline ($p < 0.05$) in the CAT activity was observed in *C. vulgaris* cells treated with 5–25 mg L^{-1} of Sm/ZnO (Fig. 7e, f).

Non-enzymatic antioxidants such as phenolics and flavonoids have also been reported to play substantial roles in the detoxification of metal and NP-induced ROS (Michalak 2006; Poborilova et al. 2013). According to our results, a significant decline in total phenolic contents was detected in the algal cells treated with 15–25 mg L^{-1} of ZnO NPs compared to the control cells (Fig. 7g). However, the concentrations of 10–25 mg L^{-1} of Sm/ZnO NPs caused more drastic reduction in the total phenolic contents in comparison to the control cells (Fig. 7h). The experiments designated a statically significant effect of 10–25 mg L^{-1} of ZnO NP treatments on the total flavonoid contents. In comparison, flavonoid contents extremely decreased after exposure to the all applied dosages of Sm/ZnO NPs (Fig. 7i, j).

Different types of stress are responsible for the induction of defense mechanisms including enzymatic and non-enzymatic antioxidant defense systems in algae. Algal cells possess several enzymes such as CAT, SOD, and APX to overcome these stresses by scavenging and eliminating the ROS (Ahmad et al. 2018). The results of the antioxidant enzyme activity assays showed that oxidative

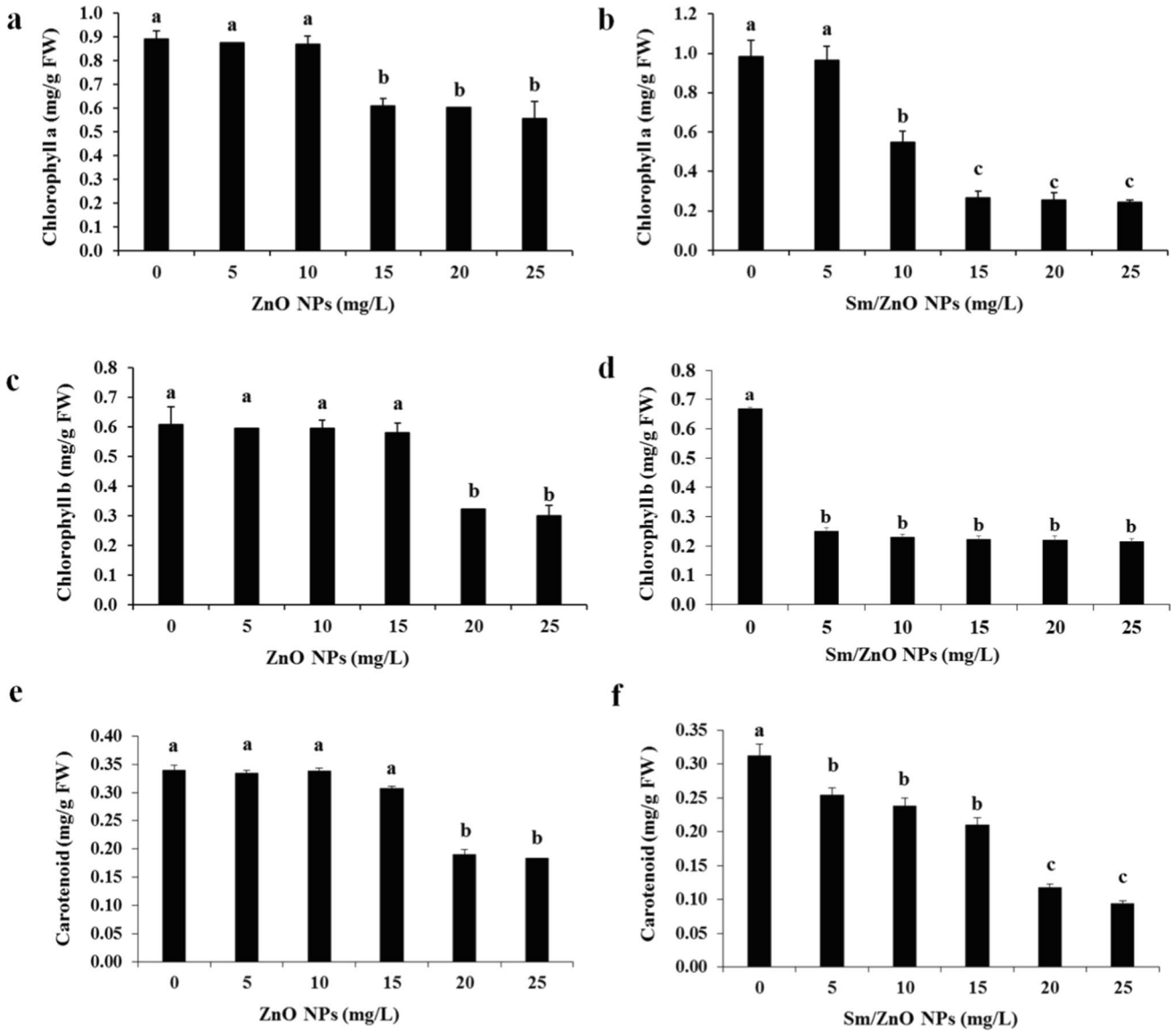

Fig. 5 Effects of ZnO (a, c, e) and Sm/ZnO NPs (b, d, f) on the photosynthetic pigment contents in *C. vulgaris* after 24 h of exposure

stress was augmented by increasing the concentrations of both ZnO and Sm/ZnO NPs in *C. vulgaris* cells. The stimulated activity of SOD and APX by ZnO and Sm/ZnO NPs in *C. vulgaris* suggested the dynamic role of these enzymes in depolluting ROS. It seems that the elevated SOD activity led to an excessive H_2O_2 generation, which subsequently enhanced APX activity inside the cells. A similar procedure has been reported for *C. vulgaris* exposed to ZnO NPs. For example, an oxidative stress induction evaluated by SOD activity has been reported in *C. vulgaris* cells treated with 300 mg L^{-1} of ZnO NPs for 72 h (Suman et al. 2015). In the case of CAT, the algal cells responded inversely to ZnO and Sm/ZnO NPs. Significant elevation of CAT activity was found in the cells treated with ZnO NPs, while reduced activity of CAT was evident in the cells exposed to Sm/ZnO NPs. The difference of CAT response in the algal cells treated with ZnO and Sm/ZnO NPs can be ascribed to the possibility of the disruption of defense mechanisms because of Sm dopant. In addition, CAT biosynthesis was possibly inhibited under the oxidative stress caused by Sm/ZnO NPs. The decline of CAT activity was suggested to be a general response to the stress probably as a consequence of the inhibition of enzyme production or an alteration in the assembly of the enzyme sub-units (Qureshi et al. 2007). Considering that APX has higher affinity for H_2O_2 than CAT, and thus they most probably act as distinct parts of different protective strategies towards scavenging of H_2O_2

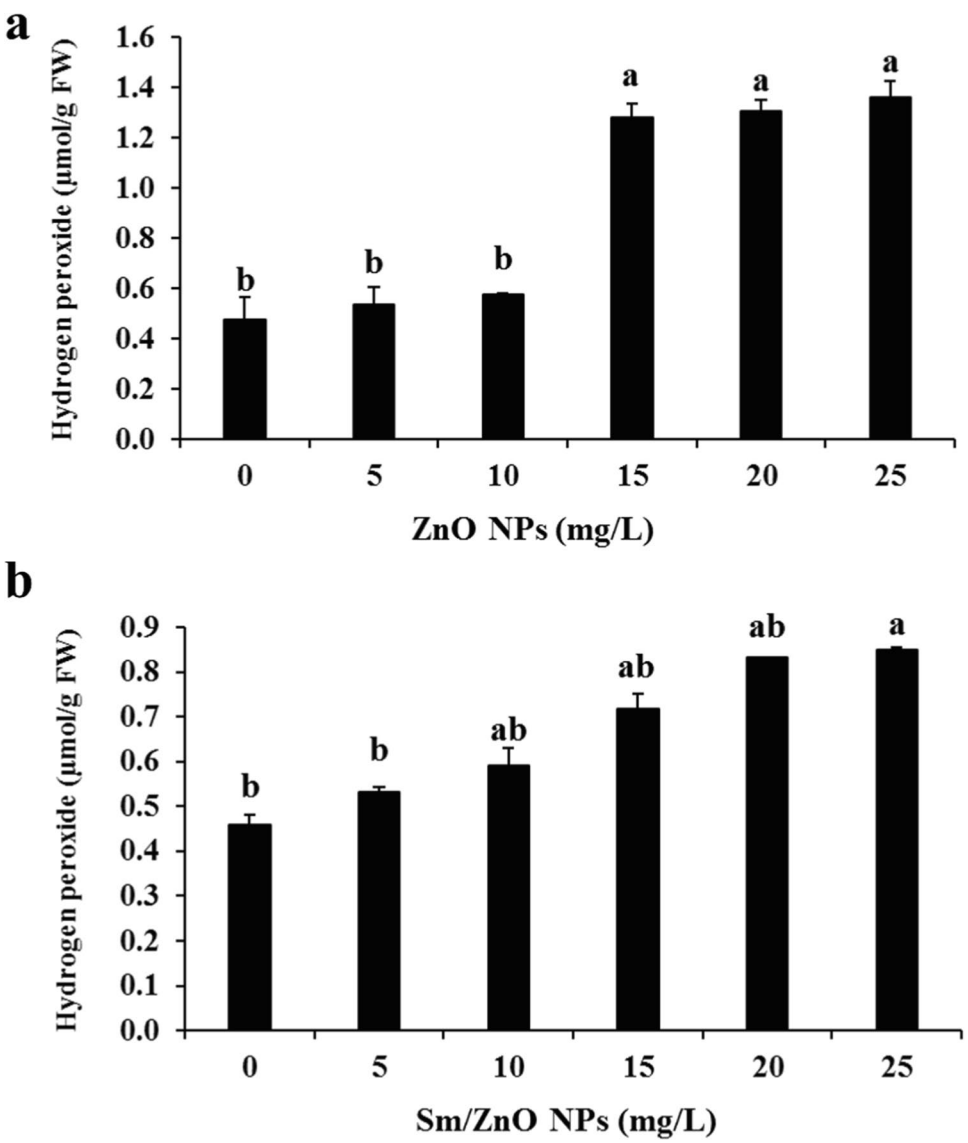

Fig. 6 H_2O_2 amount in *C. vulgaris* cells after 24 h exposure to ZnO (a) and Sm/ZnO (b) NPs

during stress conditions caused by ZnO and Sm/ZnO NPs. It seems that APX may have a more essential function throughout the stressful circumstances (Fazelian et al. 2019). Disruption in non-enzymatic defense mechanism was also identified in *C. vulgaris* cells as an outcome of ZnO and Sm/ZnO NPs exposure. Induced reduction in the non-enzymatic compounds in *C. vulgaris* cells by ZnO and Sm/ZnO NPs is in accordance with previous reports on the different NP phytotoxicity (Navarro et al. 2008; Mahjouri et al. 2018). Our results established that exposure of the algal cells to ZnO and Sm/ZnO NPs triggered a drastic oxidative stress in *C. vulgaris* cells. Although the enzymatic defense system was engaged as an essential part of protective mechanism, it was obviously not sufficient and accumulation of ROS caused oxidative damages by disruption in the enzymatic and non-enzymatic defense systems.

Conclusion

Because algae are one of the most important microorganisms in the aquatic food chain, the negative impacts of pollutants on their structure and function may have subsequent adverse effects on higher trophic levels. The present study has been designed to investigate the ecotoxicological behavior of pure and Sm-doped ZnO NPs to the green microalga *C. vulgaris* as a model biosystem. Exposure to both ZnO and Sm/ZnO NPs caused a concentration-dependent cytotoxicity confirmed by reducing the cell growth, decreasing amount of photosynthetic pigments, inducing cellular deformation, and changes in the antioxidant enzyme activities. Altogether, the obtained results confirmed the higher toxicity of Sm-doped ZnO NPs to algal cells in comparison to the undoped counterparts. Further investigations are needed to explore the

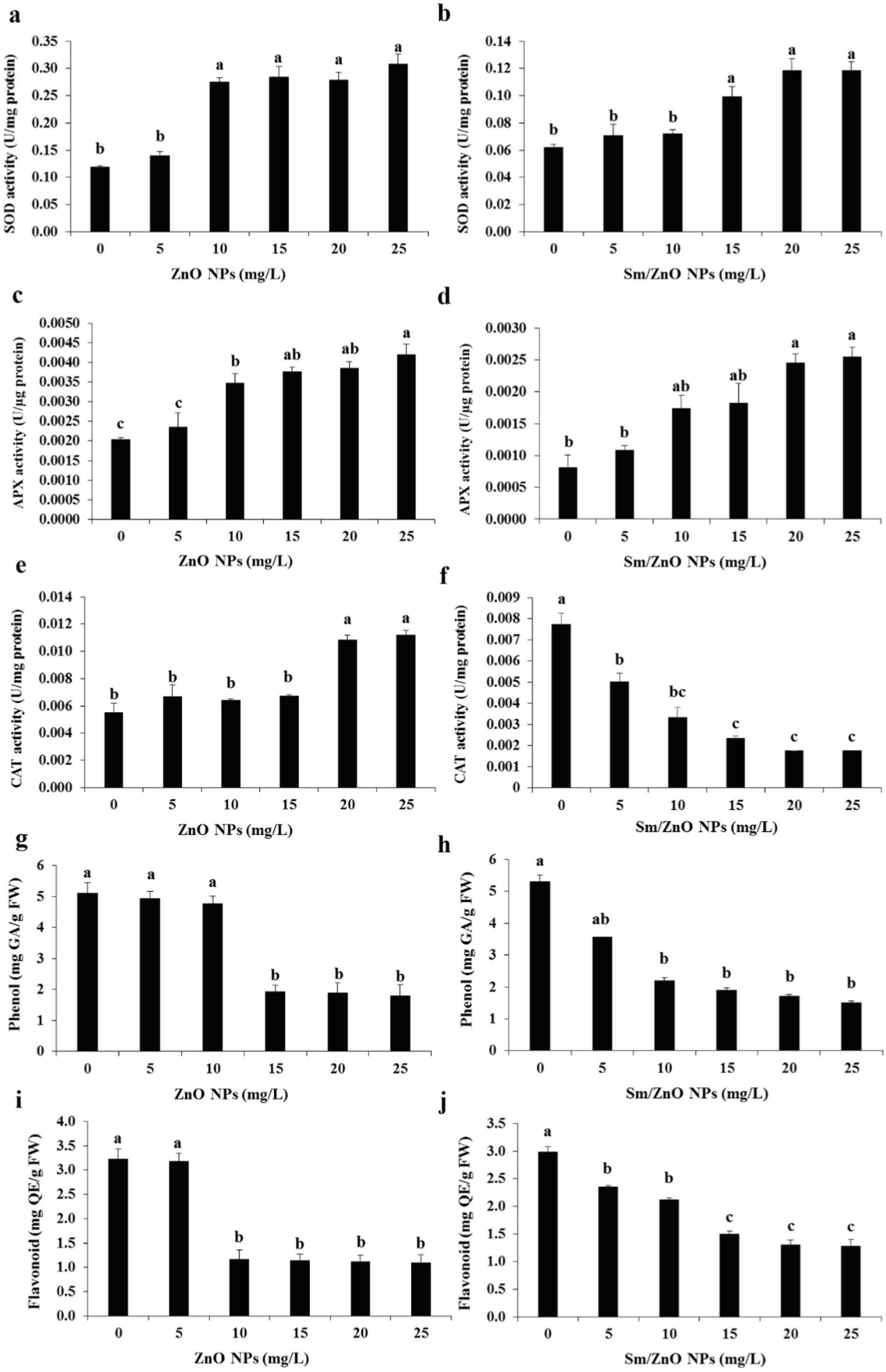
a
SOD activity (U/mg protein)
ZnO NPs (mg/L)
b
SOD activity (U/mg protein)
Sm/ZnO NPs (mg/L)
c
APX activity (U/µg protein)
ZnO NPs (mg/L)
d
APX activity (U/µg protein)
Sm/ZnO NPs (mg/L)
e
CAT activity (U/mg protein)
ZnO NPs (mg/L)
f
CAT activity (U/mg protein)
Sm/ZnO NPs (mg/L)
g
Phenol (mg GA/g FW)
ZnO NPs (mg/L)
h
Phenol (mg GA/g FW)
Sm/ZnO NPs (mg/L)
i
Flavonoid (mg QE/g FW)
ZnO NPs (mg/L)
j
Flavonoid (mg QE/g FW)
Sm/ZnO NPs (mg/L)

◂**Fig. 7** Effect of ZnO and Sm/ZnO NPs on the response of enzymatic and non-enzymatic antioxidant defense systems. Activity of SOD (a, b), APX (c, d), and CAT (e, f) enzymes as well as content of phenolics (g, h) and flavonoids (i, j) in treated *C. vulgaris* cells after 24 h of exposure

mechanisms of ZnO and Sm/ZnO NPs toxicity. Moreover, their environmental fate and behavior in the aquatic ecosystem should be determined carefully.

Acknowledgements The authors thank the University of Tabriz (Iran) for scientific and financial supports. They are also grateful to Dr. N. Farsad for his help in the statistical data analysis.

Author contribution S. Feizi, M. Kosari-Nasab, and A. Movafeghi designed the experiments. S. Feizi conducted the experiments. B. Divband helped in the synthesis and characterization of nanoparticles. M. Kosari-Nasab and A. Movafeghi controlled the methodology of microalgae culture and bioassays. S. Mahjouri and A. Movafeghi contributed to the data analysis, writing, review, and editing of the manuscript. All authors read and approved the final manuscript.

Data availability All data generated or analyzed during this study are included in the manuscript file.

Declarations

Ethics approval and consent to participate Not applicable.

Consent for publication Not applicable.

Competing interests The authors declare no competing interests.

References

Ahmad HR, Zia-ur-Rehman M, Sohail MI, ulHaq MA, Khalid H, Ayub MA, Ishaq G (2018) Effects of rare earth oxide nanoparticles on plants. In: Tripathi DK, Ahmad P, Sharma S, Chauhan DK, Dubey NK (eds) Nanomaterials in plants, algae, and microorganisms: Concepts and Controversies. Elsevier, pp 239–275

Bhuvaneshwari M, Iswarya V, Archanaa S, Madhu G, Kumar GS, Nagarajan R, Chandrasekaran N, Mukherjee A (2015) Cytotoxicity of ZnO NPs towards fresh water algae *Scenedesmus obliquus* at low exposure concentrations in UV-C, visible and dark conditions. Aquat Toxicol 162:29–38. https://doi.org/10.1016/j.aquatox.2015.03.004

Boominathan R, Doran PM (2002) Ni-induced oxidative stress in roots of the Ni hyperaccumulator, Alyssum bertolonii. New Phytol 156:205–215. https://doi.org/10.1046/j.1469-8137.2002.00506.x

Bradford MM (1976) A rapid and sensitive method for the quantitation of microgram quantities of protein utilizing the principle of protein-dye binding. Anal Biochem 72:248–254. https://doi.org/10.1016/0003-2697(76)90527-3

Carofiglio M, Barui S, Cauda V, Laurenti M (2020) Doped zinc oxide nanoparticles: Synthesis, characterization and potential use in nanomedicine. Appl Sci 10:5194. https://doi.org/10.3390/app10155194

Chang C-C, Yang M-H, Wen H-M, Chern J-C (2002) Estimation of total flavonoid content in propolis by two complementary colorimetric methods. J Food Drug Anal 10:178–182

Cheloni G, Marti E, Slaveykova VI (2016) Interactive effects of copper oxide nanoparticles and light to green alga Chlamydomonas reinhardtii. Aquat Toxicol 170:120–128. https://doi.org/10.1016/j.aquatox.2015.11.018

Chen P, Powell BA, Mortimer M, Ke PC (2012) Adaptive interactions between zinc oxide nanoparticles and Chlorella sp. Environ Sci Technol 46:12178–12185. https://doi.org/10.1021/es303303g

Djearamane S, Lim YM, Wong LS, Lee PF (2019) Cellular accumulation and cytotoxic effects of zinc oxide nanoparticles in microalga Haematococcus pluvialis. PeerJ 7:e7582. https://doi.org/10.7717/peerj.7582

Farooqi MMH, Srivastava RK (2016) Enhanced UV–vis photoconductivity and photoluminescence by doping of samarium in ZnO nanostructures synthesized by solid state reaction method. Optik 127:3991–3998. https://doi.org/10.1016/j.ijleo.2016.01.074

Fazelian N, Movafeghi A, Yousefzadi M, Rahimzadeh M (2019) Cytotoxic impacts of CuO nanoparticles on the marine microalga Nannochloropsis oculata. Environ Sci Pollut Res 26:17499–17511. https://doi.org/10.1007/s11356-019-05130-0

Goecke F, Zachleder V, Vítová M (2015) Rare earth elements and algae: physiological effects, biorefinery and recycling. In: Prokop A, Bajpai R, Zappi M (eds) Algal Biorefineries. Springer, Cham, pp 339–363

Gong N, Shao K, Feng W, Lin Z, Liang C, Sun Y (2011) Biotoxicity of nickel oxide nanoparticles and bio-remediation by microalgae Chlorella vulgaris. Chemosphere 83:510–516. https://doi.org/10.1016/j.chemosphere.2010.12.059

Hoecke KV, Quik JT, Mankiewicz-Boczek J, Schamphelaere KAD, Elsaesser A, Meeren PVd, Barnes C, McKerr G, Howard CV, Meent DVD (2009) Fate and effects of CeO_2 nanoparticles in aquatic ecotoxicity tests. Environ Sci Technol 43:4537–4546. https://doi.org/10.1021/es9002444

Kaliamurthi S, Selvaraj G, Cakmak ZE, Korkmaz AD, Cakmak T (2019) The relationship between Chlorella sp. and zinc oxide nanoparticles: changes in biochemical, oxygen evolution, and lipid production ability. Process Biochem 85:43–50. https://doi.org/10.1016/j.procbio.2019.06.005

Kayani ZN, Sahar M, Riaz S, Naseem S, Saddiqe Z (2020) Enhanced magnetic, antibacterial and optical properties of Sm doped ZnO thin films: role of Sm doping. Opt Mater 108:110457. https://doi.org/10.1016/j.optmat.2020.110457

Khatamian M, Khandar A, Divband B, Haghighi M, Ebrahimiasl S (2012) Heterogeneous photocatalytic degradation of 4-nitrophenol in aqueous suspension by Ln (La^{3+}, Nd^{3+} or Sm^{3+}) doped ZnO nanoparticles. J Mol Catal A Chem 365:120–127. https://doi.org/10.1016/j.molcata.2012.08.018

Krzyżewska I, Kyzioł-Komosińska J, Rosik-Dulewska C, Czupioł J, Antoszczyszyn-Szpicka P (2016) Inorganic nanomaterials in the aquatic environment: behavior, toxicity, and interaction with environmental elements. Arch Environ Prot 42. https://doi.org/10.1515/aep-2016-0011

Kurvet I, Juganson K, Vija H, Sihtmäe M, Blinova I, Syvertsen-Wiig G, Kahru A (2017) Toxicity of nine (doped) rare earth metal oxides and respective individual metals to aquatic microorganisms Vibrio fischeri and Tetrahymena thermophila. Materials 10:754. https://doi.org/10.3390/ma10070754

Liu N, Wang Y, Ge F, Liu S, Xiao H (2018) Antagonistic effect of nano-ZnO and cetyltrimethyl ammonium chloride on the growth of Chlorella vulgaris: dissolution and accumulation of nano-ZnO. Chemosphere 196:566–574. https://doi.org/10.1016/j.chemosphere.2017.12.184

Ma S, Lin D (2013) The biophysicochemical interactions at the interfaces between nanoparticles and aquatic organisms: adsorption and internalization. Environ Sci Proc Imp 15:145–160. https://doi.org/10.1039/C2EM30637A

Ma S, Zhou K, Yang K, Lin D (2015) Heteroagglomeration of oxide nanoparticles with algal cells: effects of particle type, ionic strength and pH. Environ Sci Technol 49:932–939. https://doi.org/10.1021/es504730k

Mahjouri S, Kosari-Nasab M, Kazemi EM, Divband B, Movafeghi A (2020) Effect of Ag-doping on cytotoxicity of SnO_2 nanoparticles in tobacco cell cultures. J Hazard Mater 381:121012. https://doi.org/10.1016/j.jhazmat.2019.121012

Mahjouri S, Movafeghi A, Divband B, Kosari-Nasab M (2018) Toxicity impacts of chemically and biologically synthesized CuO nanoparticles on cell suspension cultures of Nicotiana tabacum. Plant Cell Tissue Organ Cult 135:223–234. https://doi.org/10.1007/s11240-018-1458-x

Manzo S, Miglietta ML, Rametta G, Buono S, Di Francia G (2013) Toxic effects of ZnO nanoparticles towards marine algae *Dunaliella tertiolecta*. Sci Total Environ 445:371–376. https://doi.org/10.1016/j.scitotenv.2012.12.051

Meda A, Lamien CE, Romito M, Millogo J, Nacoulma OG (2005) Determination of the total phenolic, flavonoid and proline contents in Burkina Fasan honey, as well as their radical scavenging activity. Food Chem 91:571–577. https://doi.org/10.1016/j.foodchem.2004.10.006

Michalak A (2006) Phenolic compounds and their antioxidant activity in plants growing under heavy metal stress. Pol J Environ Stud 15:523–530

Mishra PK, Mishra H, Ekielski A, Talegaonkar S, Vaidya B (2017) Zinc oxide nanoparticles: a promising nanomaterial for biomedical applications. Drug Discov Today 22:1825–1834. https://doi.org/10.1016/j.drudis.2017.08.006

Navarro E, Piccapietra F, Wagner B, Marconi F, Kaegi R, Odzak N, Sigg L, Behra R (2008) Toxicity of silver nanoparticles to Chlamydomonas reinhardtii. Environ Sci Technol 42:8959–8964. https://doi.org/10.1021/es801785m

Nazari F, Movafeghi A, Jafarirad S, Kosari-Nasab M, Divband B (2018) Synthesis of reduced graphene oxide-silver nanocomposites and assessing their toxicity on the green microalga Chlorella vulgaris. Bionanoscience 8:997–1007. https://doi.org/10.1007/s12668-018-0561-0

Obinger C, Maj M, Nicholls P, Loewen P (1997) Activity, peroxide compound formation, and heme d synthesis in Escherichia coli HPII catalase. Arch Biochem Biophys 342:58–67. https://doi.org/10.1006/abbi.1997.9988

Peng C, Zhang W, Gao H, Li Y, Tong X, Li K, Zhu X, Wang Y, Chen Y (2017) Behavior and potential impacts of metal-based engineered nanoparticles in aquatic environments. Nanomaterials 7:21. https://doi.org/10.3390/nano7010021

Poborilova Z, Opatrilova R, Babula P (2013) Toxicity of aluminium oxide nanoparticles demonstrated using a BY-2 plant cell suspension culture model. Environ Exp Bot 91:1–11. https://doi.org/10.1016/j.envexpbot.2013.03.002

Qureshi M, Abdin M, Qadir S, Iqbal M (2007) Lead-induced oxidative stress and metabolic alterations in Cassia angustifolia Vahl. Biol Plant 51:121–128. https://doi.org/10.1007/s10535-007-0024-x

Ravichandran A, Karthick R, Xavier AR, Chandramohan R, Mantha S (2017) Influence of Sm doped ZnO nanoparticles with enhanced photoluminescence and antibacterial efficiency. J Mater Sci: Mater Electron 28:6643–6648. https://doi.org/10.1007/s10854-017-6355-2

Rippka R, Deruelles J, Waterbury JB, Herdman M, Stanier RY (1979) Generic assignments, strain histories and properties of pure cultures of cyanobacteria. Microbiology 111:1–61. https://doi.org/10.1099/00221287-111-1-1

Saxena P, Saharan V, Baroliya PK, Gour VS, Rai MK (2021) Mechanism of nanotoxicity in Chlorella vulgaris exposed to zinc and iron oxide. Toxicol Rep 8:724–731. https://doi.org/10.1016/j.toxrep.2021.03.023

Silva A, Figueiredo SA, Sales MG, Delerue-Matos C (2009) Ecotoxicity tests using the green algae Chlorella vulgaris—a useful tool in hazardous effluents management. J Hazard Mater 167:179–185. https://doi.org/10.1016/j.jhazmat.2008.12.102

Sin J-C, Lam S-M, Lee K-T, Mohamed AR (2013) Photocatalytic performance of novel samarium-doped spherical-like ZnO hierarchical nanostructures under visible light irradiation for 2, 4-dichlorophenol degradation. J Colloid Interface Sci 401:40–49. https://doi.org/10.1016/j.jcis.2013.03.043

Şükran D, GÜNEŞ T, Sivaci R (1998) Spectrophotometric determination of chlorophyll-A, B and total carotenoid contents of some algae species using different solvents. Turk J Botany 22:13–18

Suman T, Rajasree SR, Kirubagaran R (2015) Evaluation of zinc oxide nanoparticles toxicity on marine algae Chlorella vulgaris through flow cytometric, cytotoxicity and oxidative stress analysis. Ecotoxicol Environ Saf 113:23–30. https://doi.org/10.1016/j.ecoenv.2014.11.015

Tang Y, Xin H, Yang S, Guo M, Malkoske T, Yin D, Xia S (2018) Environmental risks of ZnO nanoparticle exposure on Microcystis aeruginosa: toxic effects and environmental feedback. Aquat Toxicol 204:19–26. https://doi.org/10.1016/j.aquatox.2018.08.010

Taylor NS, Merrifield R, Williams TD, Chipman JK, Lead JR, Viant MR (2016) Molecular toxicity of cerium oxide nanoparticles to the freshwater alga Chlamydomonas reinhardtii is associated with supra-environmental exposure concentrations. Nanotoxicol 10:32–41. https://doi.org/10.3109/17435390.2014.1002868

Velikova V, Yordanov I, Edreva A (2000) Oxidative stress and some antioxidant systems in acid rain-treated bean plants: protective role of exogenous polyamines. Plant Sci 151:59–66

Winterbourn CC, McGrath BM, Carrell RW (1976) Reactions involving superoxide and normal and unstable haemoglobins. Biochem J 155:493–502. https://doi.org/10.1042/bj1550493

Xia B, Liu K, Gong Z, Zheng B, Zhang X, Fan B (2009) Rapid toxicity prediction of organic chemicals to Chlorella vulgaris using quantitative structure–activity relationships methods. Ecotoxicol Environ Saf 72:787–794. https://doi.org/10.1016/j.ecoenv.2008.09.002

Yingjun W, Hangbiao J, Shihuai D, Yan C, You Y (2011) Effects of neodymium on growth and physiological characteristics of Microcystis aeruginosa. J Rare Earth 29:388–395. https://doi.org/10.1016/S1002-0721(10)60466-8

Yuan X-Z, Pan G, Chen H, Tian B-H (2009) Phosphorus fixation in lake sediments using $LaCl_3$-modified clays. Ecol Eng 35:1599–1602. https://doi.org/10.1016/j.ecoleng.2008.08.002

Zhao J, Cao X, Liu X, Wang Z, Zhang C, White JC, Xing B (2016) Interactions of CuO nanoparticles with the algae Chlorella pyrenoidosa: adhesion, uptake, and toxicity. Nanotoxicology 10:1297–1305. https://doi.org/10.1080/17435390.2016.1206149

Zhou H, Wang X, Zhou Y, Yao H, Ahmad F (2014) Evaluation of the toxicity of ZnO nanoparticles to Chlorella vulgaris by use of the chiral perturbation approach. Anal Bioanal Chem 406:3689–3695. https://doi.org/10.1007/s00216-014-7773-0

Zhu Y, Liu X, Hu Y, Wang R, Chen M, Wu J, Wang Y, Kang S, Sun Y, Zhu M (2019) Behavior, remediation effect and toxicity of nanomaterials in water environments. Environ Res 174:54–60. https://doi.org/10.1016/j.envres.2019.04.014